Spontaneous Development of Plasmacytoid Tumors in Mice with Defective Fas–Fas Ligand Interactions

By Wendy F. Davidson,* Thomas Giese,* and Torgny N. Fredrickson‡

*From the *Laboratory of Genetics and the ‡Registry of Experimental Cancers, National Cancer Institute, National Institutes of Health, Bethesda, Maryland 20892*

Summary

B cell malignancies arise with increased frequency in aging individuals and in patients with genetic or acquired immunodeficiency (e.g., AIDS) or autoimmune diseases. The mechanisms of lymphomagenesis in these individuals are poorly understood. In this report we investigated the possibility that mutations at the *Fas* (*lpr*) and *Fasl* (*gld*) loci, which prevent Fas-mediated apoptosis and cause an early onset benign lymphoid hyperplasia and autoimmunity, also predispose mice to malignant lymphomas later in life. Up to 6 mo of age, hyperplasia in *lpr* and *gld* mice results from the predominant accumulation of polyclonal T cell subsets and smaller numbers of polyclonal B cells and plasma cells. Here, we examined C3H-*lpr*, C3H-*gld*, and BALB-*gld* mice 6–15 mo of age for the emergence of clonal T and B cell populations and found that a significant proportion of aging mice exclusively developed B cell malignancies with many of the hallmarks of immunodeficiency-associated B lymphomas. By 1 yr of age, ~60% of BALB-*gld* and 30% of C3H-*gld* mice had monoclonal B cell populations that grew and metastasized in *scid* recipients but in most cases were rejected by immunocompetent mice. The tumors developed in a milieu greatly enriched for plasma cells, $CD23^-$ B cells and immunodeficient memory T cells and variably depleted of $B220^+$ DN T cells. Growth factor–independent cell lines were established from five of the tumors. The majority of the tumors were $CD23^-$ and IgH isotype switched and a high proportion was $CD5^+$ and dull Mac-1^+. Considering their Ig secretion and morphology in vivo, most tumors were classified as malignant plasmacytoid lymphomas. The delayed development of the *gld* tumors indicated that genetic defects in addition to the *Fas*/*Fasl* mutations were necessary for malignant transformation. Interestingly, none of the tumors showed changes in the genomic organization of *c-Myc* but many had one or more somatically-acquired MuLV proviral integrations that were transmitted in *scid* passages and cell lines. Therefore, insertional mutagenesis may be a mechanism for transformation in *gld* B cells. Our panel of in vivo passaged and in vitro adapted *gld* lymphomas will be a valuable tool for the future identification of genetic abnormalities associated with B cell transformation in aging and autoimmune mice.

Key words: lpr • gld • Fas • Fas ligand • lymphoma

The recessive mutant genes, *lpr* and *gld*, map to the *Fas* and *Fasl* (ligand) loci, respectively (1, 2). In normal mice, *Fas* encodes a 45-kD cell surface receptor (Fas/CD95/APO-1) belonging to the TNF/NGF receptor family and *Fasl* encodes a 40-kD type II membrane protein, FasL, homologous to members of the TNF family (1–5). In receptive cells, the aggregation of Fas receptors by FasL or anti-Fas mAb leads to the induction of cell death by apoptosis (6–8). Mice bearing the *lpr* mutation have a defect in the expression of Fas caused by the insertion of a retroviral transposon into the second intron of *Fas* that prevents normal transcription of the gene (1, 3). In *gld* mice, a point mutation in the COOH-terminal region of *Fasl* results in the expression of a non-functional form of FasL on the cell surface (2, 4). Defective interactions between Fas and FasL in mice homozygous for *lpr* or *gld* lead to indistinguishable, progressive diseases typified by profound lymphadenopathy, splenomegaly, high titers of circulating autoantibodies, hypergammaglobulinemia, strain-dependent systemic autoimmune disease and premature death (reviewed in reference 9). Recently, there have been several reports of pediatric patients with a variety of genetic mutations at the *FAS* locus and a spectrum of immune abnormalities closely resembling those of *lpr* and *gld* mice (10–14). The consistency of the immunologic defects associated with *Fas* mutations suggests a universal role for the Fas-associated cell deletion

pathway in regulating lymphocyte survival and in preventing the accumulation of autoreactive B cells.

Between 1 and 6 mo of age, the spleens and lymph nodes of *lpr* and *gld* mice undergo progressive enlargement associated with the accumulation of two functionally unresponsive $B220^+$ T cell subsets not detected in normal mice. Lymphadenopathy results predominantly from the selective amassing of non-transformed $B220^+CD4^-CD8^-$ double negative ($B220^+DN$)[1] T cells (9, 15). The majority of these cells are derived from $CD8^+$ precursors selected in the thymus on MHC class I Ag (16–19). The other $B220^+$ T cell subset is a minor one that expresses low levels of CD4 and arises independently of MHC class I expression (16–20). As the $B220^+$ T cells accumulate, they dilute conventional $CD4^+$ and $CD8^+$ T cells and B cells and disrupt the normal architecture of the spleen and LN. Although normal T and B lymphocytes are reduced by proportion, their total numbers in LN are increased approximately 10-fold (21, 22). The expanded $CD4^+$ and $CD8^+$ T cell populations in 4–6-mo-old *lpr* and *gld* mice are greatly enriched for memory-like cells (9, 20–23). Similarly, the B cell population is enriched for cells with the phenotype of chronically activated B cells and for Ig-secreting cells (9, 24). The skewing of the T and B cell populations towards primed and activated cells is consistent with the demonstrated role of Fas-mediated apoptosis in regulating the survival of Ag-activated T cells and autoreactive B cells (25–29). For C3H-*gld*, C3H-*lpr* and BALB-*gld* mice whose median lifespans are ~12 mo, lymphoproliferative disease persists until death but the cellular composition of the lymphoid tissues in aging mice has not been extensively studied.

Although defective Fas–FasL interactions in *lpr* and *gld* mice lead to the accumulation of massive numbers of lymphocytes, there have been no reports of malignant T or B lineage tumors arising in these mice. In unpublished studies involving the transfer of spleen cells from BALB-*gld* mice with advanced disease into immunodeficient CB.17-*scid* mice, we observed that a significant number of recipients developed malignant B cell lymphomas of donor origin. To further investigate the possibility that *gld* mice spontaneously develop lymphomas that are masked by the preexisting lymphoproliferative disease, we surveyed groups of C3H-*gld* and BALB-*gld* mice of various ages for evidence of clonal, transformed lymphoid populations. These studies revealed that by 1 yr of age, 28% of C3H-*gld* mice and 57% of BALB-*gld* mice had monoclonal outgrowths of B cells in spleen and LN. After transfer into *scid* recipients, the majority of these clonal B cell populations gave rise to metastatic plasmacytoid tumors. These findings provide evidence that in addition to limiting the accumulation of polyclonally activated and autoreactive lymphocytes, normal Fas–FasL interactions also prevent the development of B cell neoplasms.

[1] *Abbreviations used in this paper:* ALPS, autoimmune lymphoproliferative syndrome; DN, double negative; IAL, immunodeficiency-associated lymphomas; MAIDS, mouse AIDS; RT, room temperature.

Materials and Methods

Mice. All mice were bred and maintained at PerImmune, (Rockville, MD; National Cancer Institute contract NOI CB-710-85). C3H-*lpr/lpr* (C3H-*lpr*) and C3H-*gld/gld* (C3H-*gld*) mice were bred from breeding pairs obtained from The Jackson Laboratory (Bar Harbor, ME). BALB/c-*gld/gld* (BALB-*gld*) mice were bred in our colonies from C3H-*gld* mice backcrossed for 15 generations to BALB/cAnPt mice. C3H-*scid/scid* mice breeding pairs were obtained from Sprague Dawley (San Diego, CA) and C.B-17-*scid/scid* breeding pairs were the gift of Dr. D. Hilbert (NCI, NIH, Bethesda MD). For tumor transfer studies, *scid* recipients were injected i.p. with 1 to 2×10^7 donor spleen or LN cells. Tumor-bearing mice were palpated weekly and killed 2–6 wk post-transplant before they became moribund.

Characterization of Tumors. Lymphoid tissues from mice bearing primary tumors or from *scid* mice with tumor transplants were processed for histology, FACS® analysis, and in vitro culture. Tumor cells were viably frozen and cell pellets were snap frozen for DNA and RNA extraction. Cell lines were established from spleen or LN cells from *scid* mice with tumor transplants. The lines were maintained in complete RPMI 1640 with 10% fetal bovine serum.

DNA Analyses. High MW DNA was isolated, digested with EcoRI, HindIII, HpaI or PvuII (Boehringer Mannheim, Indianapolis, IN), separated on 0.7% agarose gels and blotted onto Nytran membranes (Schleicher & Schuell, Keene, NH) using established techniques. Probes used included J_{11}, a 1.96-kb BamHI–EcoRI fragment of the BALB/c germline J_H region (30); IVS, a 1.1-kb EcoRI–Xba fragment of the BALB/c germline C_κ region (31); CT_β, a 618 bp BamHI–EcoRI fragment containing the J and C regions of 86TI (32), a cDNA clone coding for the β-chain of the T cell receptor; pEco, a 400-bp SmaI fragment derived from an AKR ecotropic virus *env* gene (33); and pvt, a 1.4-kb EcoRI fragment of the germline *Pvt1* (34). The *c-Myc* probe was a 1.3-kb fragment containing exon 2 and exon 3 (gift from Dr. K. Huppi, NCI, NIH, Bethesda, MD). The probes were ^{32}P-labeled by nick translation (Lofstrand, Rockville, MD). Washings of Southern blots were done to a final stringency of 0.1× SSC, 0.5% SDS at 65°C.

FACS® Analyses. Single cell suspensions of spleen and LN were prepared, blocked with anti-CD32 mAb, and stained as described previously (15). Analyses were performed on a FACScan® (Becton Dickinson, Sunnyvale, CA). Dead cells were eliminated from the analysis by propidium iodide gating. Abs used for staining included various combinations of Tri-color (TC)-labeled anti-CD45(B220), anti-CD8 (Caltag, San Francisco, CA), PE-labeled mAb specific for CD4, IgL κ, IgL λ, CD45(B220), CD8, CD32, CD19, and CD95(Fas) and FITC-labeled mAb specific for TCR-α/β, ThB, CD11b (Mac-1), CD23, CD80 (B7-1), CD86 (B7-2), 6C3 (Ly-6C), CD43, I-A^k, I-A^d, CD5, IgM, IgG1, IgG2b, IgG2a, and IgG3 (PharMingen, San Diego, CA).

Preparation of Tissues for Histology. Tissues were fixed in modified Tellyesniczky's solution and processed at American Histolab, Gaithersburg, MD.

Quantitation of Anti-ds-DNA Autoantibodies in Sera. 96-well flat bottomed microtiter plates were coated with 10 μg/ml methylated BSA (Sigma Chemical Co., St. Louis, MO) in carbonate buffer (pH 9.6) overnight at 4°C. After washing with PBS/0.05% Tween 20, the plates were incubated with 10 μg/ml calf thymus DNA in carbonate buffer overnight at 4°C. The plates were blocked with dilution buffer containing 2% PEG 8000, 1% gelatine, 0.05% Tween 20, 1% BSA in PBS for 30 min. at 37°C. Serum samples

were diluted twofold starting at 1:500 in diluting buffer, added to the plates, and incubated for 2 h at 37°C. Anti-DNA Ab binding was detected with biotinylated anti-mouse IgG (Southern Biotechnology) and POD-labeled streptavidin using ABTS as the substrate.

Quantitation of Serum Ig Levels. Levels of IgM, IgG1, IgG2a, IgG2b, IgG3, and IgA in sera were determined by ELISA. ELISA plates were coated overnight at 4°C with 50 μl of goat antibodies specific for mouse IgM, IgA, IgG2a, IgG2b, and IgG3 diluted to 5 μg/ml or 50 μg/ml (IgG3) in carbonate buffer (KPL, Gaithersburg, MD). After washing the plates were blocked with 200 μl of SuperBlock (Pierce Chemical Co., Rockford, IL) for 20 min at room temperature (RT). Ig standards and serial dilutions of mouse sera (50 μl) in blocking buffer were added and the plates were incubated for 2 h at RT. After washing the plates with PBS-Tween, 100 μl of the following detecting mAb labeled directly with HRP or AKP were added to the appropriate wells. Anti-IgG2a (R19-15) 1:1,000, anti-IgG2b (R12-13) 1:2,000, anti-IgG3 (R40-82) 1:100, anti-IgA (R6-60.2) 1:1,000, and anti-IgM (R5-140) 1:1,000 (PharMingen). The plates were incubated for 1.5 h at RT then washed with PBS-Tween. The HRP or AKP substrates (KPL, Gaithersburg, MD) were added, the reaction was stopped and the plates were read.

Results

Evidence for the Outgrowth of Clonal B Cell Populations in 11–15-mo-old BALB-gld and C3H-gld Mice. To further investigate the possibility that defects in the Fas–FasL-mediated cell death pathway may predispose mice to the development of B cell lymphomas, we surveyed groups of 4–8-mo-old and 9–16-mo-old BALB-*gld* and C3H-*gld* mice for tumor incidence. All mice had advanced lymphoproliferative disease and the majority were not moribund at the time of death. For each mouse, lymphoid and nonlymphoid tissues were processed for histologic analysis, spleen, and lymph node were analyzed by FACS® for the distribution of lymphocyte subsets, DNA was extracted from spleen and LN and examined for evidence of clonal expansion of cells with rearranged IgH, IgL, or TCR genes, and fresh or viably frozen lymphoid cell suspensions were transferred into immunodeficient *scid* recipients. Similar analyses also were performed on groups of 25 $BALB^{+/+}$ and $C3H^{+/+}$ control mice 10–25 mo of age. The results of Southern blot analyses of DNA for IgH and IgL gene rearrangements are summarized in Table 1. For both BALB-*gld* and C3H-*gld* mice, there is strong evidence for an age-related accumulation of cells with clonal IgH and IgL rearrangements in both spleen and LN. Among DNA samples from a total of 46 9–15-mo-old BALB-*gld* mice, 39 (85%) had one or more prominent rearranged IgH and IgL bands, three (6%) had rearranged IgH bands only, and four (9%) had no detectable rearranged bands.

Of the 39 samples with clonal IgH and IgL rearrangements, 26 (67%) had between one to three prominent rearranged IgH and IgL bands common to spleen and LN suggesting the selective outgrowth of one or two B cell clones. Fig. 1 shows typical examples of members of this group. Except for sample 540, only data for LN DNA is shown, but in each case, identical bands also were present in spleen. The remaining thirteen samples had four or more rearranged IgH and IgL bands suggesting the accumulation of oligoclonal B cell populations (Table 1). Potential monoclonal/biclonal B cell populations also were detected in the spleens of 2/12 4–8-mo-old BALB-*gld* mice (Table 1).

Among 68 11–15-mo-old C3H-*gld* mice examined, 28% (19/68) had outgrowths of monoclonal/biclonal B cell populations in spleen and LN, 15% (10/68) had oligoclonal B cell populations and the remainder (57%) had no detectable clonal outgrowths (Table 1). Typical examples of C3H-*gld* mice with potential monoclonal/biclonal B cell populations in spleen and LN are shown in Fig. 2. In contrast to the 4–8-mo-old BALB-*gld* mice, no clonally expanded B cell populations were detected in the spleens or LNs of 4–8-mo-old C3H-*gld* mice (Table 1).

The accumulation of clonal B cell populations with age is not restricted to *gld* mice. The incidence of monoclonal/biclonal and oligoclonal B cell populations in the spleen and LN of 25 11–15-mo-old C3H-*lpr* mice paralleled that for age-matched C3H-*gld* mice (Table 1). In contrast, no clonal outgrowths of cells with IgH or IgL rearrangements were detected in the spleens of 12 to 15 mo old control $C3H^{+/+}$ or $BALB^{+/+}$ mice by Southern blot analyses and there was no histologic evidence of tumor development in these mice (Fig. 3 and data not shown). In spite of the massive accumulation of T cells in *lpr* and *gld* mice, populations of cells with clonal rearrangements of TCR-β genes were not detected in the spleen or LN at any age (data not shown).

Monoclonal B Cell Populations from BALB-gld and C3H-gld Mice Grow and Metastasize in scid Recipients. To determine

Table 1. *Outgrowth of Clonal B Cell Populations in C3H-lpr, C3H-gld, and BALB-gld Mice*

Strain	Age Range	Number of mice	IgH and IgL gene rearrangements		
			Mono- or biclonal*	Oligoclonal‡	None§
	mo				
BALB-*gld*	4–8	12	2	3	7
	9–15	46‖	26	13	4
$BALB^{+/+}$	10–21	22	0	0	22
C3H-*gld*	4–8	9	0	0	9
	11–15	68	19	10	39
C3H-*lpr*	11–15	25	8	4	14
$C3H^{+/+}$	11–15	25	0	0	25

*Spleen and LN cell DNA with ≤4 prominent rearranged clonal IgH and IgL bands.
‡Spleen and LN cell DNA with >4 rearranged IgH and IgL bands.
§No detectable clonal rearrangements.
‖Three mice had rearranged IgH bands without detectable rearranged IgL bands.

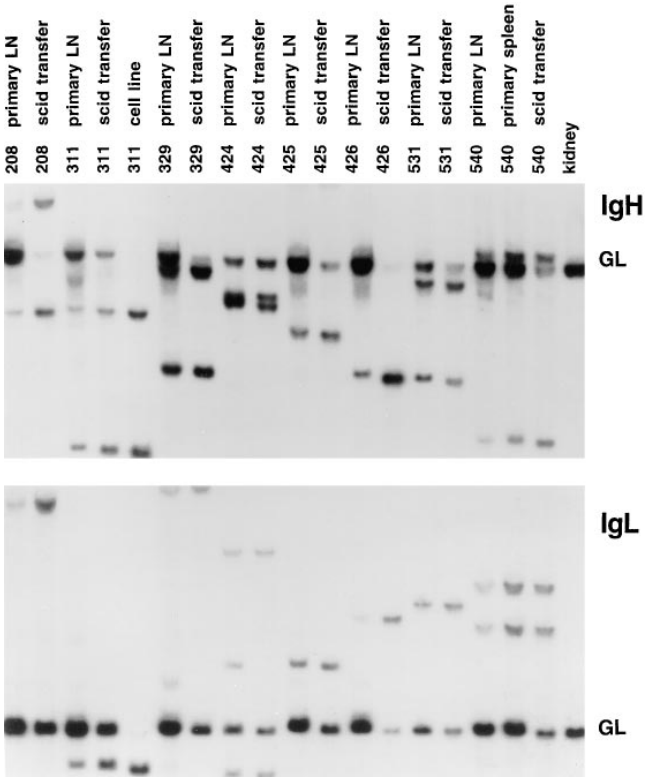

Figure 1. Evidence for the development of monoclonal/biclonal B lineage tumors in aging BALB-*gld* mice. Top and bottom panels show Southern blot analyses of genomic DNA isolated from the LN of representative 8 to 12 mo old BALB-*gld* mice bearing primary tumors, and from the LN of C.B-17-*scid* mice bearing the corresponding transplanted tumor (primary transplant). Data also are shown for splenic DNA from the primary 540 tumor and for DNA from the 311 cell line. In the top panel, DNA was digested with EcoRI and examined for rearrangement of the IgH locus with the pJ11 probe. In the bottom panel, DNA was digested with HindIII and examined for rearrangement of the IgL locus with the IVS probe. GL, indicates the position of the unrearranged germline IgH and IgL bands in BALB-*gld* kidney DNA (lane *19*).

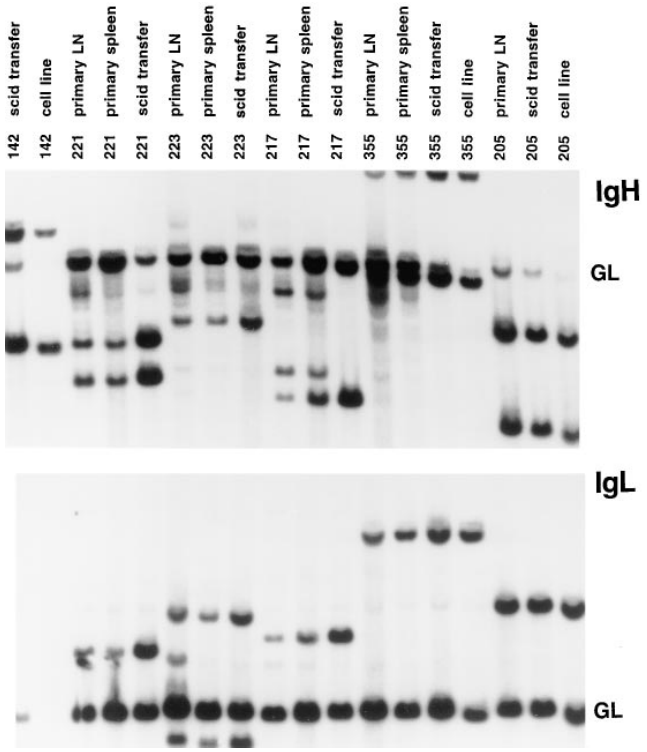

Figure 2. Evidence for the development of monoclonal/biclonal B lineage tumors in aging C3H-*gld* mice. Panels show Southern blot analyses of genomic DNA for IgH (*top*) and IgL (*bottom*) gene rearrangements (see Fig. 1 legend for details). DNA samples isolated from the spleen and LN of C3H-*gld* bearing primary tumors, from the LN of C3H-*scid* mice bearing primary tumor transplants and from cell lines are compared. GL indicates the position of the germline IgH and IgL bands.

if the monoclonal/biclonal B cell populations accumulating with age in the BALB-*gld* and C3H-*gld* mice were transplantable, fresh or viably frozen spleen or LN cells were injected intraperitoneally into histocompatible immunodeficient *scid* recipients. Of 23 suspected tumors inoculated, twenty gave rise to metastatic monoclonal B lineage tumors 3–8 wk after inoculation. As shown in Figs. 1 and 2, each tumor transplant had identically rearranged IgH and IgL bands to the clonal B cell populations in the primary inoculum. In one C3H-*gld* mouse, 217, at least two B cell clones were present originally but only one grew out consistently in *scid* mice (Fig. 2). The tumors showed some variations in their growth patterns in adoptive transfers. The C3H-*gld* tumor 355 grew very aggressively in all lymphoid organs. All of the other tumors grew rapidly in the spleen, mesentery, mediastinal and mesenteric LN and more slowly in peripheral LN. The majority of the tumors metastasized to the liver, lungs, and kidneys. Some tumors, (e.g., C3H-*gld* tumors 142, 217, and 221 and the BALB-*gld* tumor 540) also grew in the ovaries and uterus. Only the C3H-*gld* tumors 217 and 205 induced copious production of ascites. In contrast, there was no selective outgrowth of B cells in *scid* mice injected with spleen or LN cells from *gld* or +/+ mice with no evidence of clonal B cell populations (data not shown).

The C3H-*gld* tumors 142, 205, 217, 355, and 362 were injected i.p. or s.c. into 6–8-wk-old $C3H^{+/+}$, -*gld*, and -*lpr* recipients and the BALB-*gld* tumors 311 and 208 were injected i.p. or s.c. into 6–8-wk-old $BALB^{+/+}$ and -*gld* mice to determine if they would grow in immunocompetent mice or have a growth advantage in *gld* recipients. The cells used for injection were grown in *scid* mice and were highly enriched for tumor cells. Tumor growth was assessed histologically, by FACS®, and by Southern blot analysis. Tumor 355 grew very aggressively in the peritoneal cavity, spleen, and peripheral LN in all three groups of recipients and killed the mice within 2 weeks of inoculation. Tumor 142 grew in the ovaries of 1/5 C3H-*gld* recipients but was not detected in C3H-*lpr* or $C3H^{+/+}$ mice 2 mo after injection. None of the remaining tumors grew in, or were recoverable from, any of the recipients 2–6 mo after inoculation. To determine if the tumors had a growth advantage in older mice with advanced lymphoproliferative disease, tumors 217 and 205 were injected i.p. into groups of 7 mo

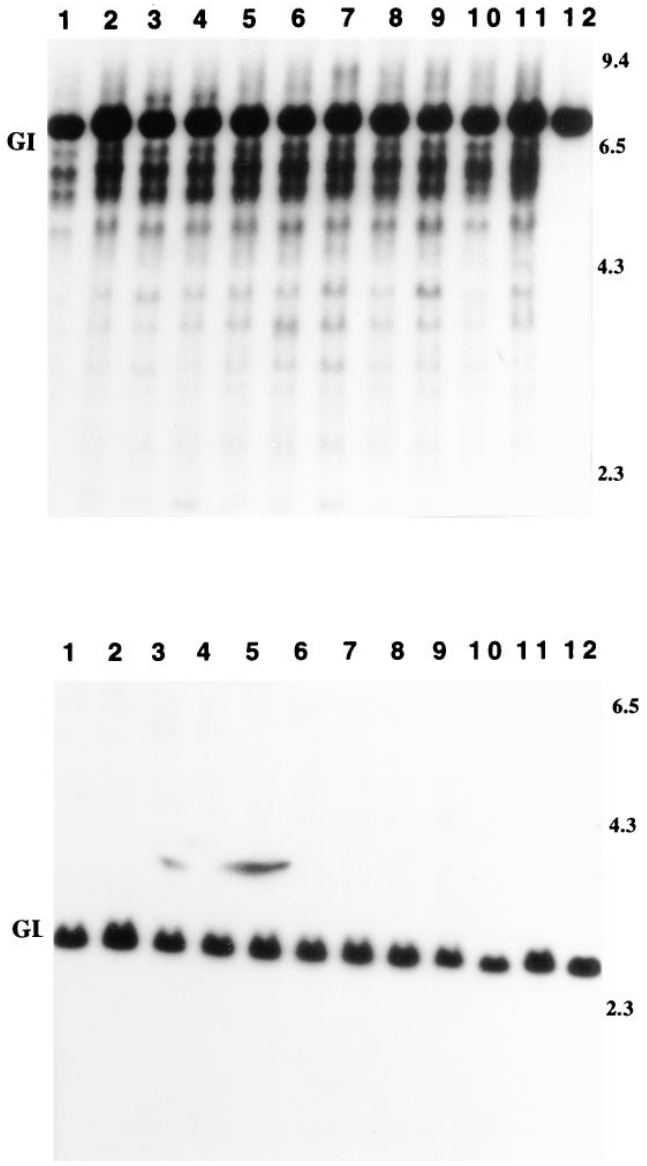

Figure 3. Clonal B cell outgrowths are not detected in the spleens of 12–15-mo-old Balb/$c^{+/+}$ mice. Panels show Southern blot analyses of genomic DNA for IgH (*top*) and IgL (*bottom*) gene rearrangements. DNA was isolated from the spleens of 12–15-mo-old Balb/$c^{+/+}$ (lanes *1–11*) or from Balb/$c^{+/+}$ kidney (lane *12*). GL indicates the position of the germline IgH and IgL bands. Data are representative of 25 mice analyzed.

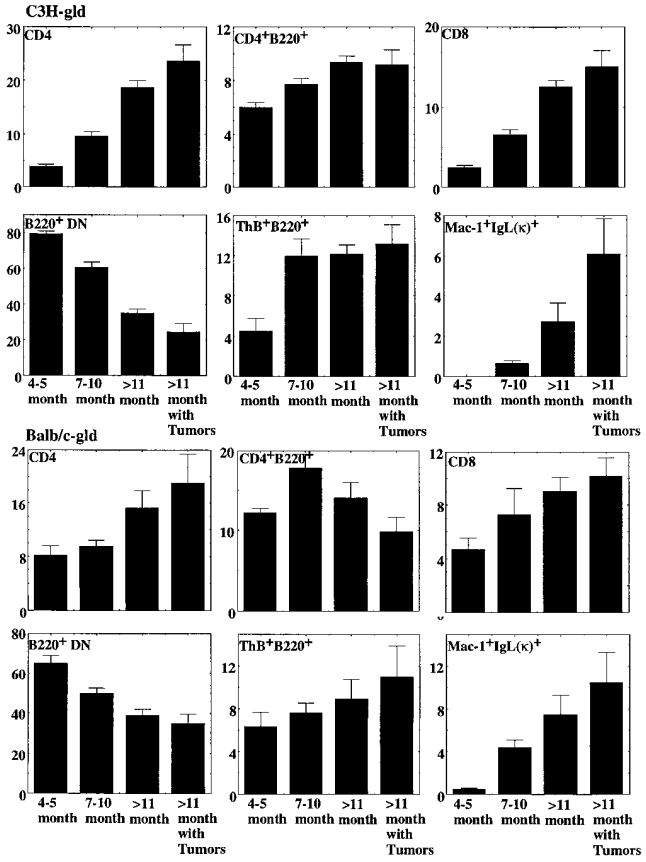

Figure 4. Age-related changes in the distribution of T and B cell subsets in the LN of C3H-*gld* and BALB-*gld* mice. The percentage of each lymphocyte subset (identified in top right hand corner) was determined by 3-color FACS® analysis of LN cells from individual BALB-*gld* and C3H-*gld* mice aged 4–5 mo, 7–10 mo, and >11 mo. Data is shown for all mice >11 mo and mice >11 mo with tumors. The proportions of $B220^+$ DN T cells were determined by staining cells with PE-labeled anti-CD4 and anti-CD8, Tri-color-conjugated anti-CD45(B220), and FITC-labeled anti-TCR-α/β. The histograms represent the mean plus SE of values for 11 to 68 C3H-*gld* mice (top six panels) and 11–23 BALB-*gld* mice (bottom six panels).

old *lpr* mice and the mice were killed 2 mo later. No tumor growth was detected in any of the recipients (data not shown).

Age-related Changes in the Cellular Composition of Lymphoid Organs in gld Mice. The BALB-*gld* mice used in this study have not been described previously. These mice developed progressive lymphoproliferative disease closely resembling that of C3H-*gld* mice in terms of time of onset, severity, and pathology. At 4–5 mo of age, when lymphadenopathy and splenomegaly were well established and comparable in both strains, some consistent but minor strain-related differences were observed in the proportions of the various T cell subsets. As shown in Fig. 4, $B220^+$ DN T cells predominated in the LN of both strains of mice at 4–5 mo of age but the BALB-*gld* mice had lower proportions of this subset and higher proportions of $CD4^+$ T cells, $CD4^+$ $B220^+$ T cells and $CD8^+$ T cells than the C3H-*gld* mice. Between 6 mo and ~1 yr of age, a previously unreported redistribution of lymphocyte subsets occurred in the LN of both BALB-*gld* and C3H-*gld* mice. This was more apparent in the C3H-*gld* mice and was characterized by a selective decrease in the proportions of $B220^+$ DN T cells from 79.5 ± 1.4% to 35.1 ± 2.1%, and a three- to fourfold increase in the proportions of $CD4^+$ T cells, $CD8^+$ T cells and B cells (Fig. 4). A small 1.6-fold increase in the proportion of $CD4^+B220^+$ T cells also was observed (Fig. 4). Spleens from aging C3H-*gld* mice and LN and spleens from aging BALB-*gld* mice showed a similar pattern of changes in the distribution of T cell subsets (Fig. 4 and data not shown). These changes in cellular composition were not

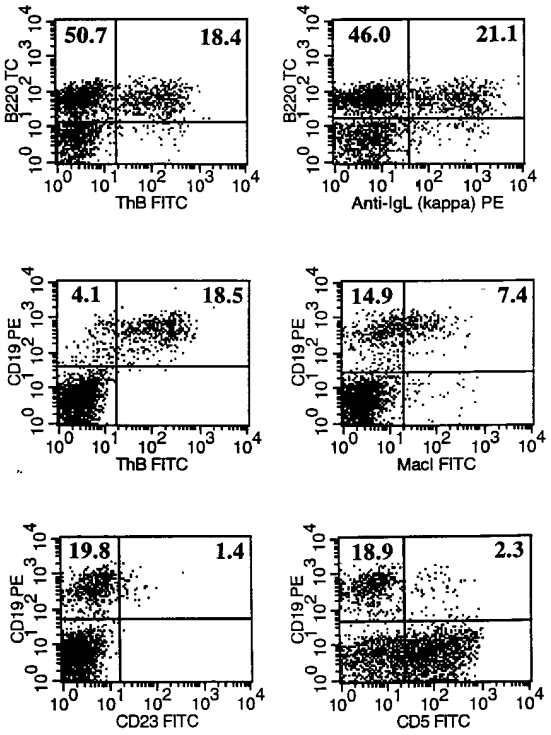

Figure 5. Age-related accumulation of $B220^+CD19^+ThB^+kappa^+$ $CD23^-$ B cells in *gld* mice. LN cells from a 12-mo-old BALB-*gld* mouse with no detectable tumor were stained with the reagents indicated. Values inside the quadrants represent the proportions of positive cells. Two thirds of the $CD19^+$ B cells were Mac-1^- and one third expressed low levels of Mac-1.

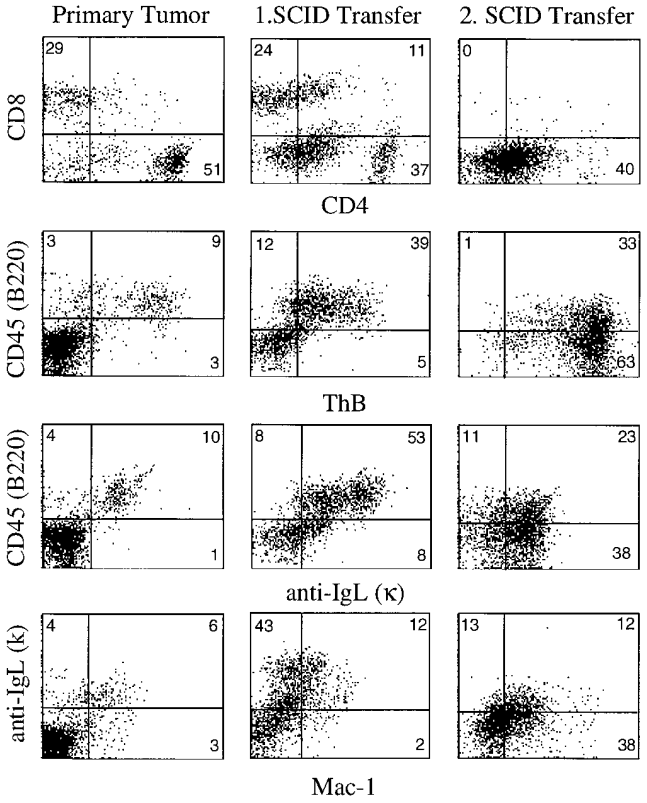

Figure 6. Phenotype of the C3H-*gld* tumor, 217 in vivo. Panels on the right hand side show FACS® data for LN cells from the mouse bearing the primary tumor 217. The adjacent panels show corresponding data for LN cells from C3H-*scid* mice bearing the primary (*center*) and secondary (*right*) 217 transplants. Cells were stained with the reagents indicated and analyzed on the FACScan®. The values inside each quadrant represent the percentage of reactive cells.

accompanied by a reduction in LN or spleen size or cellularity and did not correlate with the development of B lineage tumors (Fig. 4 and data not shown). Among the B cells, there was an age-related increase in the proportions and numbers of $kappa^+B220^+CD19^+ThB^+CD5^-CD23^-$ cells. By ~1 yr of age, the majority of the B cells in LN and spleen were of this phenotype (Fig. 5). Among these cells, a subset also expressed low to intermediate levels of Mac-1 (Figs. 4 and 5). In LN, the Mac-1^+ subset represented fewer than 0.5% of cells at 4–5 mo of age and by ~1 yr of age had increased to 2.7 ± 0.9% in C3H-*gld* and 7.5 ± 1.8% in BALB-*gld* mice. Between 4 and ~12 mo of age, the proportions of Mac-1^+ B cells in spleen increased from 1.6 ± 0.3% to 5.0 ± 0.4% for C3H-*gld* mice and from 2.6 ± 0.5% to 9.8 ± 1.4% for BALB-*gld* mice. In contrast, this subset represented fewer than 3% of the cells in the spleens of 11–15-mo-old $C3H^{+/+}$ and $BALB^{+/+}$ mice (data not shown). Although the accumulation of $CD23^-$ Mac-1^+ B cells was greatest in tumor-bearing mice, animals lacking tumors also had significantly increased proportions of these cells (Figs. 4 and 5 and data not shown).

Comparisons of the Phenotypes of the Primary Tumors and scid-propagated Tumors. Among the tumor bearing mice, Ig^+ B cells rarely exceeded 10–20% of the total population in LN and spleen and the tumor population was not readily identified by a unique phenotype or selective increase in size. Therefore, accurate phenotyping and morphologic classification of the tumors was dependent on their selective outgrowth in *scid* transplants. This is illustrated in Fig. 6 for tumor 217 which is representative of the majority of the tumors isolated. The LN of the mouse bearing the primary tumor had 29% $CD8^+$ T cells, 36% $CD4^+B220^-$ T cells, 11% $CD4^+B220^+$T cells, 2% $B220^+$DN T cells and 10% $\kappa^+B220^+ThB^+$ B cells (Fig. 6 and data not shown). Approximately 60% of the B cells in LN and spleen expressed low levels of Mac-1. Transfer of these LN cells into *scid* mice resulted in an aggressive outgrowth of donor cells in the spleen and mesenteric LN, cellular infiltration of nonlymphoid organs, and the production of ascites. In a typical recipient, 40% of the cells in LN were $kappa^+IgG3^+B220^+ThB^+Ia^+CD5^+$ $CD80^+CD86^+Fas^+$ B cells and 38% of these expressed low levels of Mac-1 (Fig. 6 and data not shown). The whole B cell population also reacted weakly with anti-CD4 mAb (Fig. 6). B cells with a similar phenotype represented 64% of the spleen cells (data not shown). With a few exceptions, the primary *scid* transplants of the remaining C3H-*gld* and BALB-*gld* tumors had phenotypes closely resembling 217. All of the tumors expressed intermediate to high levels of B220, Ia, CD16/32,

Table 2. *Tumor Surface and Secreted Ig Isotypes*

Tumor	Surface Ig*	Secreted Ig‡	*Myc/Pvt 1* rearrangements§
C3H-*gld*			
142	IgG2a	IgG2a	ND‖
205	Null	IgG2a	ND
217	IgG3	IgG3	ND
221	Null	IgA	ND
223	IgG3	IgG3	ND
355	Null	IgG2a	ND
362	Null	IgG3	ND
BALB-*gld*			
208	IgG1	IgG1	ND
311	Null	IgG3	ND
329	IgM	IgM	ND
421	IgM	IgM	ND
424	IgA	IgA	ND
425	IgG2a	IgG2a	ND
426	IgA	IgA	ND
536	IgA	IgA	ND
540	IgG2a	IgG2a	ND

*Surface Ig expression on *scid*-passaged tumor cells determined by FACS® analysis.
‡Isotype of secreted Ig in sera from tumor-bearing *scid* mice determined by ELISA assay.
§Rearrangement of *Myc* and *Pvt1* loci determined by Southern blot analysis of genomic DNA from *scid*-passaged tumors.
‖ND, not detected. Rearrangements of *Myc* or *Pvt1* were not detected.

CD19, CD80, and CD86 and levels of ThB ranging from low to high. Only 355 was Fas^-. Most of the tumors were $CD23^-$ and expressed low to intermediate levels of CD5 and low levels of Mac-1. Five tumors, 142, 205, 355, 362, and 311, were consistently sIg^- and the remainder had low to intermediate levels of IgH and IgL chains. With the exception of 142 which was λ^+, all sIg^+ tumors expressed kappa L chains. A variety of IgH isotypes were expressed including IgM, IgG1, IgG2a, IgG3, and IgA (Table 2). Sera from the majority of the *scid* mice transplanted with Ig^+ C3H-*gld* and BALB-*gld* tumors had high titers of Ig of the same isotype expressed on the tumor (Table 2). The surface Ig^- tumors growing in *scid* mice also secreted Ig of a single isotype (Table 2). Notably, none of the sera reacted with ds-DNA (Table 2). In many instances, the primary tumors also appeared to be secreting Ig as one or two gamma spikes were detected in electrophoreses of sera from 66% (19/29) of tumor-bearing mice (data not shown). Histologically, the tumor populations in the primary *scid* transfers were a mixture of immunoblasts, plasmacytoid cells and plasma cells.

Surprisingly, 40% of the LN cells in the primary *scid* transplant of 217 were T cells (28% TCR-α/β^+CD8^+T cells and 12% TCR-α/β^+CD4^+ T cells) and significantly more T cells were recovered than were present in the original inoculum. The proliferation of T cells in the first *scid* transfer was observed with many of the C3H-*gld* and BALB-*gld* tumors and was not always skewed towards $CD8^+$ T cells. Analyses of TCR-β chain gene rearrangements showed no evidence of clonality among the T cell populations in any of the *scid* recipients (data not shown). Of note, there was no significant outgrowth of $B220^+$ DN T cells or $B220^+CD4^+$ T cells in any of the *scid* mice inoculated with tumor-bearing populations.

In secondary *scid* transfers with LN cells from the primary *scid* recipients, clonal descendants of the 217 tumor cells predominated and T cells represented fewer than 3% of the cells (Fig. 6). The tumor population was enriched further for plasmacytoid cells and plasma cells as illustrated by high titers of serum IgG3 and changes in phenotype and morphology. The majority of the cells remained $IgG3^+CD45^+CD5^+ThB^+Ia^+CD80^+CD86^+Fas^+CD19^+$ dull $CD4^+$ and dull Mac-1^+ and a significant proportion downregulated their expression of surface Ig and switched from CD45(B220) expression to a lower MW CD45 isoform (Fig. 6 and data not shown). This skewing of the tumor population towards more differentiated plasmacytoid cells and plasma cells in secondary and subsequent *scid* transfers was a hallmark of the majority of the tumors arising in C3H-*gld* and BALB-*gld* mice.

Establishment and Phenotype of Tumor Cell Lines. Among the 19 tumors that grew in *scid* recipients, 5 (142, 205, 217, 355, and 311) have been adapted successfully to culture. All of the tumors propagated in *scid* mice survived for at least 2–3 wk in culture but were difficult to maintain long-term. Only 355 grew aggressively and independently from the beginning. Initially, tumors 142, 205, 217, and 311 were highly dependent on adherent stromal cell populations for their survival and these could not be substituted with IL-6. The tumor cells adhered tightly to the stromal cells and had to be trypsinized to be passaged. Subsequently, stromal cell–independent sublines were established for all four lines. These lines grow both in large clusters and as weakly adherent monolayers. Analyses of IgH and IgL gene rearrangements confirmed that each cell line was clonally related to the *scid*-transfer tumor from which it was established (Figs. 1 and 2). All of the lines grew vigorously in *scid* mice (data not shown). In general, the cell lines were phenotypically similar to the *scid*-propagated cells from which they were derived but showed changes in the level of expression of some antigens. For example, there was downregulation of the expression of ThB and CD45(B220) on the 217 line and of ThB, Fas, CD80, and CD86 on the 311 line (Fig. 7). Although T cell proliferation was often observed in the primary *scid* passages of the tumors, none of the cell lines induced the proliferation of +/+ or *gld* T cells in syngeneic mixed lymphocyte cultures (data not shown).

Histopathologic Changes in Aging C3H-gld and BALB-gld Mice. The first organs to be affected in C3H-*gld* and BALB-*gld* mice were the lymph nodes, particularly the

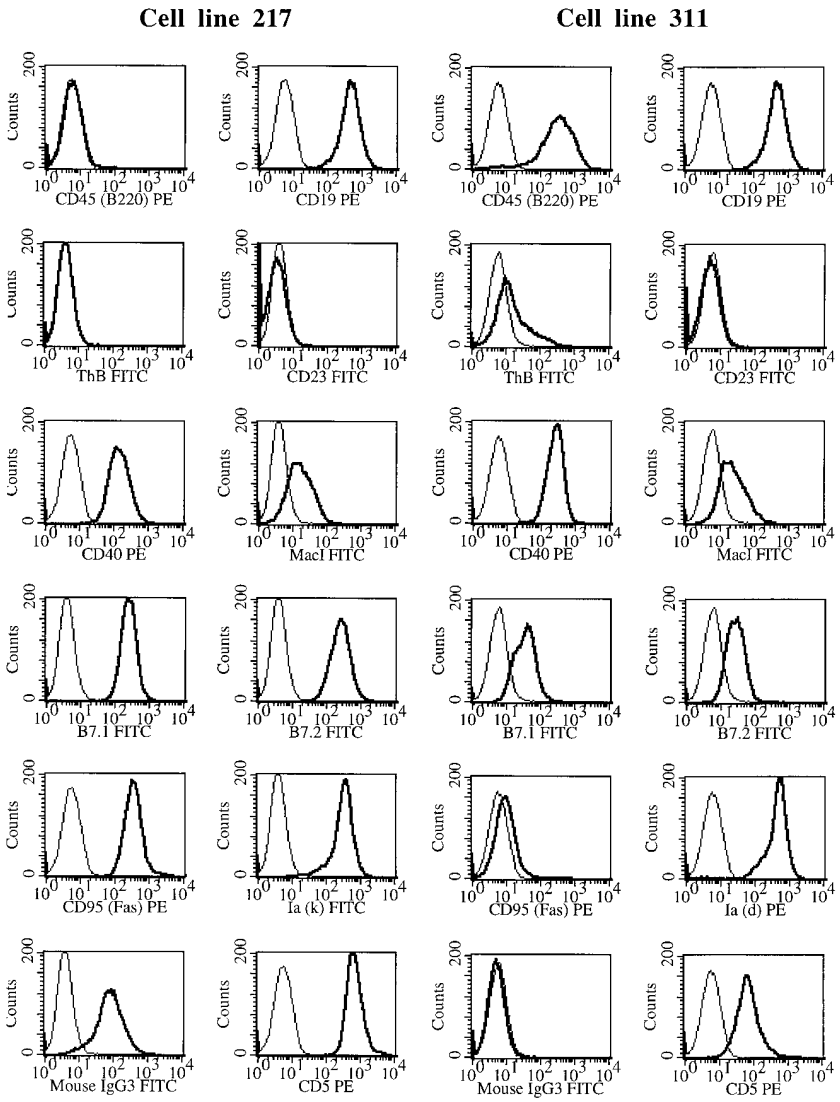

Figure 7. Cell surface marker expression on in vitro-propagated cell lines established from the C3H-*gld* tumor, 217, and the BALB-*gld* tumor, 311. Cells were stained with the antibodies indicated (*heavy lines*) or with a non-reactive FITC- or PE-conjugated control Ab (*light lines*) as described in Materials and Methods.

subcutaneous ones. Normal LN architecture was lost as the $B220^+$ DN T cells selectively accumulated. By ~4 mo of age, sheets of homogeneous medium-sized DN T cells with characteristically stippled chromatin totally replaced the cortex and expanded the medullary cords so that the sinusoids were effaced (Fig. 8 *A*). At the same time, the splenic white pulp became greatly enlarged and cells morphologically resembling the $B220^+$ DN T cells occupied both the periarteriolar sheath and the mantle zone (data not shown). In both the LN and spleen, plasmacytoid cells were present in variable numbers but they represented a small minority of cells. In the lung, periarteriolar cuffing by lymphoid cells was moderately advanced, but the kidneys and liver were unaffected at this time (data not shown).

Beyond 6 mo of age, the LN and spleen underwent further changes in cellular composition and cellular infiltration of nonlymphoid tissues was more widespread. These changes occurred in both tumor-bearing mice and mice without apparent tumors. In LN and spleen, the cells became progressively less densely packed and the stromal elements were more apparent. The homogeneous DN T cell population was replaced increasingly by small lymphocytes, immunoblasts, plasmacytoid cells, plasmablasts, and plasma cells. Consistent with a previous report by Jacobson et al. (35), the plasma cells in spleen characteristically accumulated around the central arteriole in the periarteriolar lymphoid sheaths. Infiltration, mainly by plasmacytoid cells, became increasingly severe in the lungs, portal areas of the liver, and renal medulla. Fig. 8 *B* shows typical cellular changes and plasma cell infiltrates in the LN of a 12-mo-old C3H-*gld* mouse with no detectable tumor.

The increased presence of the activated B cell populations and plasma cells, together with the underlying T cell accumulation greatly complicated the morphologic classification of the primary tumors. This difficulty is illustrated well by the prototypic tumor 217. For this tumor, there was moderate splenic and hepatic, and more severe renal infiltration. However, as shown in Fig. 8 *C* and *D*, the cells

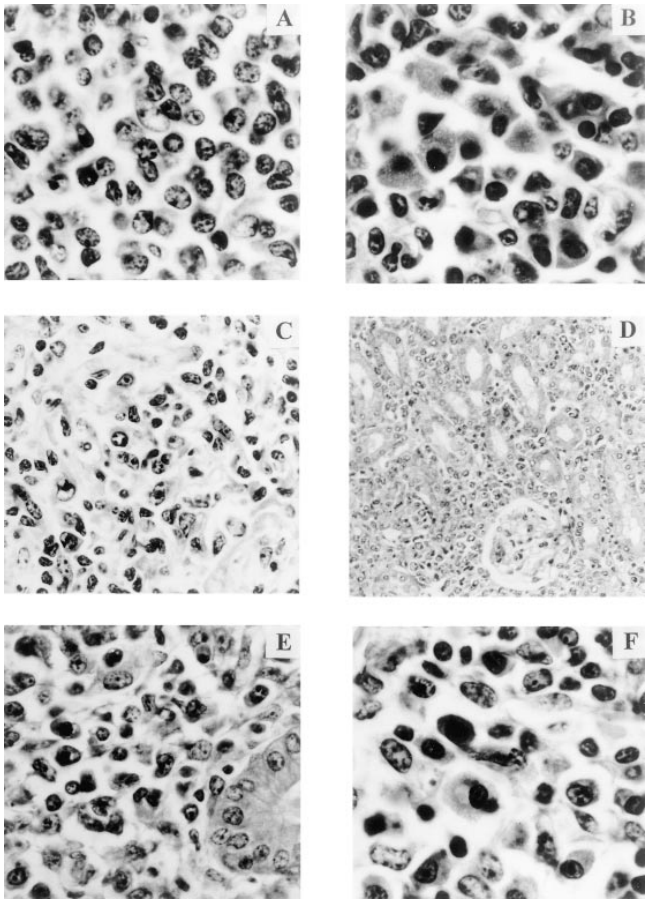

Figure 8. Malignant and nonmalignant lymphoid infiltrates in the tissues of aging *gld* mice. *A* illustrates the selective accumulation of DN T cells with characteristically stippled chromatin in a section of LN from a 4-mo-old C3H-*gld* mouse (H&E, original magnification 600×). *B* shows a typical example of the loss of the DN T cell population and the accumulation of nonmalignant plasma cells in the LN of a tumor-free 12-mo-old C3H-*gld* mouse (H&E, original magnification 600×). *C* and *D* show the morphologic heterogeneity of the cellular infiltrates in the spleen (*C*, original magnification 200×) and kidney (*D*, original magnification 100×) of the C3H-*gld* mouse bearing the primary 217 tumor. Panel E illustrates the extensive infiltration of the uterus with malignant plasmacytoid cells and plasma cells and non-malignant T lymphocytes in a C3H-*scid* mouse inoculated with the primary 217 tumor. *F* shows a LN section from a C3H-*scid* mouse bearing the second passage of tumor 217 in which the majority of the cells are monoclonal tumor cells (H&E, original magnification 600×). The mixture of immunoblasts, plasmablasts and plasma cells is typical of the morphologic heterogeneity associated with the malignant plasmacytoid *gld* lymphomas.

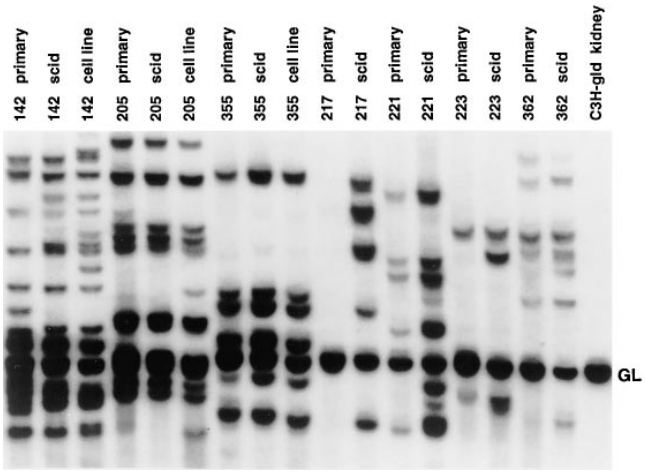

Figure 9. Evidence for somatically-acquired clonal MuLV proviral integrations in C3H-*gld* tumors. Southern blot of genomic DNA from primary tumors, *scid*-passaged tumors and tumor cell lines digested with *PvuII* and probed with a ^{32}P-labeled ecotropic MuLV probe. DNA from C3H-*gld* kidney shows the position of the single hybridizing germline (*GL*) band present in normal C3H cells.

were morphologically heterogeneous making it difficult to identify the tumor population. In the first and all subsequent passages of 217 in *scid* mice, there was extensive tumor infiltration of the lymphoid organs, lungs, liver, mesentery, perirenal fat, ovaries, and uterus and to a lesser extent kidneys. Fig. 8 *E* illustrates the intrauterine infiltration in the first *scid* passage. In the primary passage of 217 and most of the other C3H-*gld* and BALB-*gld* tumors, the infiltrating cells were a mixture of donor T cells and tumor cells but in the subsequent passages the infiltrates were composed almost exclusively of monoclonal tumor cells (Fig. 5 and data not shown). In all passages, the 217 tumor population was morphologically heterogeneous and included immunoblasts, plasmablasts and plasma cells in varying proportions (Fig. 8 *F*). All of the BALB-*gld* and most of the C3H-*gld* tumors closely resembled 217 in their patterns of growth and morphology. The exceptions among the C3H-*gld* tumors were 355, 205, and 142. Whereas these clearly were mature B cells by phenotype and Ig secretion, they were less differentiated morphologically. In summary, even though morphologic identification of the primary C3H-*gld* and BALB-*gld* tumors was difficult, their clonal descendants that proliferated in *scid* recipients almost universally were skewed towards the late stages of B cell differentiation and were classified as malignant plasmacytoid lymphomas.

C3H-gld and BALB-gld Tumors Have Somatically Acquired, Clonal MuLV Proviral Integrations. The transformation of mature B lineage cells frequently involves multiple genetic events including the dysregulated expression of cellular protooncogenes. For example, plasmacytomagenesis often is associated with dysregulated expression of *c-Myc* caused by the translocation of this gene to the switch regions of the *IgH* locus or by rearrangement of the *Pvt1* locus (34, 36). Abnormal expression of oncogenes also can occur following the insertion of infectious endogenous retroviruses into the genome (37). To determine the potential involvement of either of these mechanisms in the development of the *gld* tumors, DNA from the primary tumors, *scid* transfers and cell lines was examined for evidence of *c-Myc* translocation and proviral integrations. Rearrangement of *c-Myc* was investigated by Southern blot analysis and PCR analysis using primers specific for *c-Myc* and the μ, α, γ1, and γ2a switch regions. None of the C3H-*gld* or BALB-*gld* primary tumors, transplants or cell lines showed evidence

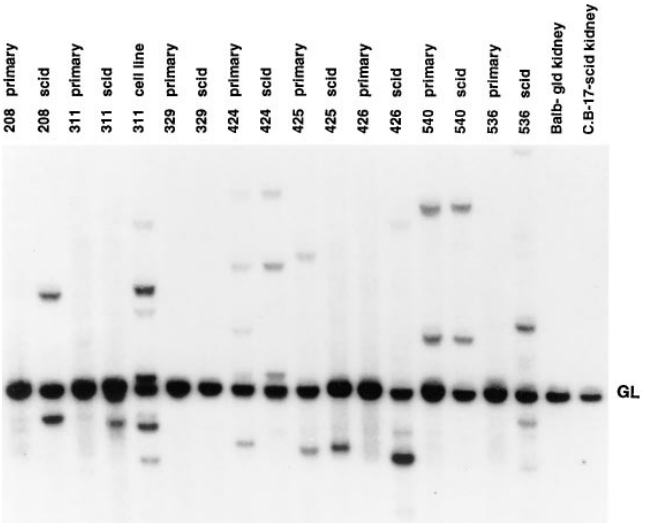

Figure 10. Somatically-acquired clonal MuLV proviral integrations in BALB-*gld* tumors. Southern blot analysis of *Pvu*II-digested genomic DNA from BALB-*gld* primary tumors, *scid* transplants and the 311 cell line. The blot was hybridized with a ^{32}P-labeled ecotropic MuLV probe. Control DNA samples from BALB-*gld* and C.B-17-*scid* kidneys show the position of the germline (*GL*) band.

of *c-Myc* translocation, or amplification or disruption of the *Pvt1* locus (data not shown).

Both C3H and BALB/c mice have single germline copies of endogenous infectious ecotropic MuLV (Figs. 9 and 10). In contrast, a high proportion of the C3H-*gld* and BALB-*gld* tumors had somatically acquired MuLV proviral integrations. As shown in Fig. 9, the transplantable C3H-*gld* tumors 142, 205, 355, 221, 223, and 362 had between 2 and 13 viral integrations in the primary tumor. 217 was the only primary tumor with no evidence of newly acquired proviral integrations. A different pattern of viral integrations was observed for the BALB-*gld* mice (Fig. 10). Among 17 monoclonal transplantable tumors surveyed, seven had newly acquired proviral integrations in both the primary and *scid*-propagated populations (e.g., 425 and 540), seven had integrations in the transplanted but not the primary tumor (e.g., 311 and 536), and three had no detectable new integrations (e.g., 329). In general, the primary BALB-*gld* tumors had many fewer somatically acquired proviral insertions than the C3H-*gld* tumors (Figs. 9 and 10). This difference is most likely explained by known differences between BALB/c and C3H mice in the genetic loci that regulate the spread of N-tropic ecotropic virus with BALB/c mice being restrictive and C3H mice permissive (38). Most of the bands in the primary C3H-*gld* and BALB-*gld* tumors also were present in the *scid* transplants and in the in vitro cell lines indicating that the majority of the proviral integrations are stable. In some cases new bands arose in the *scid* transplants and the cell lines. This is particularly evident in the *scid* transplants of 217 and 536 and in the 311 cell line (Figs. 9, 10). Although these new integrations clearly are not involved in tumor induction, they may be important for tumor progression or adaptation to culture. The great variation in the sizes of the viral bands indicate that there are few common integration sites among the tumors. It should be noted that somatically acquired ecotropic virus integrations were not detected in DNA from young *gld* mice or tumor-free aged *gld* mice (data not shown).

Discussion

This study was undertaken to examine the effects of the life-long absence of a functional Fas–FasL-mediated cell deletion pathway on spontaneous lymphomagenesis. We showed that a mutant, nonfunctional FasL significantly accelerated the onset and increased the incidence of lymphomas in C3H and BALB mice. The tumors developed in a milieu greatly enriched for plasma cells, CD23$^-$ B cells and memory-like CD4$^+$ and CD8$^+$ T cells and variably depleted of B220$^+$ DN T cells. The lymphomas were restricted to the B cell lineage, were skewed towards the terminal stages of B cell differentiation, were transplantable in immunodeficient mice, and hence were classified as malignant plasmacytoid lymphomas. The majority of the tumors were CD23$^-$ and IgH isotype switched and a high proportion were CD5$^+$ Mac-1 dull. None of the tumors showed changes in the genomic organization of c-*Myc*.

The age-related accumulation of a putatively primed or activated IgM$^+$CD23$^-$CD5$^-$ B cell subset unrelated to CD23$^-$ B-1a or B-1b cells has been reported previously for MRL-*lpr*, B6-*lpr*, and B6-*gld* mice (24). Our studies show that a similar B cell population accrues in aging C3H-*gld* and BALB-*gld* mice, and that in these strains a subset of the cells also express low levels of Mac-1. The accumulation of CD23$^-$ cells in *lpr* and *gld* mice may be a consequence of chronic B cell activation and/or increased longevity stemming from the Fas–FasL defect. If the CD23$^-$ B cells are long-lived, they may be at increased risk of transformation, and in this regard resemble the naturally long-lived B-1a and B-1b cells that give rise to lymphomas in aging NZB mice (39). The development of *gld* tumors that phenotypically resembled isotype-switched CD23$^-$ B2 cells, CD23$^-$ CD5$^+$Mac-1$^+$ B-1a cells, and CD23$^-$CD5$^-$Mac-1$^+$ B-1b cells implies that each of these B cell subsets may be susceptible to transformation in *gld* mice.

There is compelling evidence that chronic inflammatory diseases or infections resulting in persistent lymphoproliferation may be conditioning events in the development of B cell malignancies (40–42). As one example, there is a strong correlation between infection with *Helicobacter pylori* and the development of B lineage gastric lymphomas (43, 44). Although chronic infections are unlikely to be a driving force in the development of tumors in Fas–FasL-deficient mice, self antigens may be responsible for chronic B cell activation. In support of this proposal, lymphoma-bearing TCR-β/δ-deficient *lpr* mice had high titers of circulating anti-mouse IgG autoantibodies (45). In the present study, none of the *gld* tumors secreted detectable levels of anti-dsDNA autoantibodies, but a role for other autoantigens in promoting chronic B cell stimulation has not been eliminated.

Previously, we and others reported an age-related accumulation in *lpr* and *gld* mice of memory-like $CD4^+$ and $CD8^+$ T cells with the capacity to secrete high levels of IL-4, IL-10, IFN-γ, and TNF-α (20–23). These cytokines, with their well-established effects on B cell survival, proliferation and differentiation (46–49), also may promote or enhance B cell activation and contribute to the prolonged survival and accumulation of plasma cells. Paradoxically, the accumulation of memory cells in *lpr* and *gld* mice is associated with defects in the capacity of T cells to proliferate and secrete IL-2 in vitro in response to a wide variety of mitogens, and superantigens (9, 50). Skewing of the T cell population towards memory cells and losses in mitogenic responses and IL-2 production also occured in aging humans and normal 2–3 yr-old mice (51–53). In aged +/+ mice, the memory T cell population had decreased expression of Fas and a defect in FasL-induced apoptosis (53). Moreover, overexpression of Fas in CD2-*Fas*-transgenic mice prevented the age-related accumulation of immunodeficient memory cells and also delayed thymic involution (53). These observations suggest that T cell senescence is associated with defective Fas-mediated signaling and this may explain the apparent acceleration of immune senescence in *lpr* and *gld* mice.

Our finding that the majority of the *gld* B cell tumors were rejected by young +/+, *lpr* and *gld* mice, implies that the tumors were immunogenic for immunocompetent mice and that rejection was not dependent on a functional Fas-mediated apoptosis pathway. Parallel results were obtained recently in mice made T cell-deficient by inactivation of both TCR-β and TCR-δ genes. These mice normally develop IgM^+ B cell lymphomas with low incidence but tumor development was increased greatly if the mice also were homozygous for *lpr* (45). In contrast to our system, the tumors in the T cell–deficient *lpr* mice developed rapidly and ~60% of the mice had tumors by 7 mo of age (45). Interestingly, lymphomagenesis in the *lpr* mice was prevented if the mice had either TCR-α/β^+ or TCR-γ/δ^+ T cells, implying that the tumor cells were immunogenic and that in young immunocompetent mice, each T cell type was able to delete the tumor cells by a Fas-independent pathway (45). This study and ours suggest that chronic activation and enhanced survival of B cells together with defective immune surveillance contribute to accelerated lymphomagenesis in Fas–FasL-deficient mice.

A strong correlation between immunodeficiency and B cell lymphomagenesis has been reported previously in humans and mice (40–42, 54, 55). In humans, immunodeficiency resulting from treatment with immunosuppressive drugs or secondary to infection with HIV greatly increases the risk of B cell lymphoma development (41, 54, 55). Similarly, patients with congenital or age-related immunodeficiencies, with a variety of autoimmune diseases, or with angioblastic lymphoproliferative disorders have an increased risk of developing B lineage tumors (41, 54, 56). Like the *gld* tumors, human immunodeficiency-associated lymphomas (IAL) also can retain their immunogenicity. For example, IAL in organ transplant patients have been reported to spontaneously regress when immunosuppressive therapy is discontinued (41, 55).

Among mice, B lymphomas also develop with high frequency in C57BL/6 mice infected with LP-BM5 murine leukemia viruses which cause an acquired immunodeficiency syndrome designated mouse AIDS (MAIDS; 57). These aggressive IAL also can be propagated readily in *scid* mice but are rejected by immunocompetent mice (58). In another system involving C57BL/KaLwRij mice, a murine model of multiple myeloma, plasmacytomagenesis correlated strongly with an age-related T cell imunodeficiency (59, 60). Because the *gld* B lymphomas share many of the hallmarks of mouse and human IAL, we propose that they represent a novel subset of IAL that develop as a result of the complex and cumulative effects on the immune system of defective Fas–FasL interactions. These effects may include chronic Ag-driven B cell activation, the ready availability of T cell help and growth factors, the loss of a major elimination pathway for activated B cells, and an age-related deficit in T cell–dependent immune surveillance.

The increased risk of B cell lymphomagenesis associated with *Fas* and *Fasl* mutations is not restricted to mice. Recently, a family was described in which two out of four members with genomic *FAS* mutations and autoimmune lymphoproliferative syndrome (ALPS) were diagnosed with B cell lymphomas at 25 yr of age (61). In contrast, none of the reported pediatric cases of ALPS with germline *FAS* mutations has a history of lymphoma (10–14). Although the number of cases is small, the delayed development of B cell tumors in the patients is consistent with our findings in *lpr* and *gld* mice and implies that progression to malignancy is dependent on the accumulation of additional mutations in DNA. Other evidence for a possible association between *FAS* mutations and B cell malignancy comes from a recent study of patients with multiple myeloma in which *FAS* mutations were detected in 10% of tumor-containing bone marrow aspirates (62). Although we observed nonlymphoid tumors only rarely in *lpr* and *gld* mice, two of four ALPS patients described by Drappa et al. (14) developed nonlymphoid tumors in adulthood. It is not clear if these tumors arose as a result of treatment with cytotoxic drugs or infection with hepatitis virus or if *FAS* mutations generally increase the risk of neoplasia.

Little is known about the sites or mechanisms of mutation in IAL. Experimentally-induced plasmacytomas in BALB/c mice consistently have *c-Myc*-activating t(12;15) or t(6;15) translocations that are believed to be vital for the transformation process (34, 36). In contrast, our primary or passaged BALB-*gld* and C3H-*gld* plasmacytoid tumors, which often evolved into plasmacytomas in *scid* passages, had no evidence of *c-Myc* or *Pvt1* rearrangement or amplification suggesting that novel genetic mutations may substitute for *c-Myc* dysregulation in these tumors. Similarly, *c-Myc* translocations were not detected in the multiple myelomas arising in the C57BL/KaLwRij mice or in the MAIDS B cell lymphomas (58–60). In other experimental mouse models of lymphomagenesis, murine leukemia viruses have been found to induce neoplasms by integrating into the

host DNA and mutating or transcriptionally activating flanking genes (37). Our observation that a high proportion of the *gld* tumors had one or more somatically acquired proviral integrations that were stably transmitted in *scid* passages and cell lines, raises the possibility that insertional mutagenesis may be a mechanism of transformation in *gld* IAL. It is not known if interference with the Fas-mediated cell death pathway only serves to increase the pool of targets for transformation and to protect the tumors cells from Fas-mediated apoptosis, or if mutations in *Fas* or *Fasl* cooperate with other mutations. In this regard, it recently was reported that the *lpr* mutation accelerated lymphomagenesis in *Eμ-L-myc* transgenic mice but not in *Eμ-Pim-1* transgenic mice (63,64), indicating that under some circumstances cooperation may occur.

Both $BALB^{+/+}$ and $C3H^{+/+}$ mice have been reported to develop B lineage tumors, but these generally were not detected until the mice were 2–3 yr of age (65, 66). In addition, the spontaneous neoplasms of +/+ mice developed with a much lower frequency, and were more morphologically diverse than the *gld* tumors (65, 66). Consistent with the strain-related differences in tumor incidence observed in the present study, the incidence of B cell tumors in the $BALB^{+/+}$ mice was significantly higher than in the $C3H^{+/+}$ mice (66). The persistence in strain differences in tumor susceptibility in the *gld* mice, suggests that the pro-oncogenic effects of the FasL defect may complement, but not override, preexisting tumor susceptibility factors. The tumor accelerating effects of *gld* also are dependent on homozygosity as *gld*/+ mice showed no evidence of decreased lifespan or tumor development (data not shown). This contrasts with our earlier studies where we observed that SJL-*lpr*/+ mice developed B cell tumors more rapidly and died earlier than $SJL^{+/+}$ mice (67). It has yet to be determined if this effect is *lpr*-dependent, strain-dependent, or both.

The loss of $B220^+$ DN T cells with advanced age in *lpr* and *gld* mice has not been reported previously. The mechanisms leading to the depletion of these cells are unknown but may involve diminished production, or age-related exhaustion. Interestingly, $CD8^+$ T cells, which are the putative progenitors of $B220^+$ T cells (16–19), often were greatly increased in mice deficient in $B220^+$ DN T cells. One explanation for this observation is that only a subset of $CD8^+$ T cells can differentiate into $B220^+$ DN T cells and that with time these either diminish in numbers or lose their capacity to differentiate. The loss of $B220^+$ DN T cells and the development of B cell tumors appear to be coincidental events in the *lpr* and *gld* mice because many mice with greatly diminished numbers of $B220^+$ DN T cells were tumor-free and not all tumor-bearing mice were depleted of DN T cells.

In conclusion, we have shown that inactivation of the Fas-mediated cell death pathway by mutation of *Fas* or *Fasl* accelerates the development and greatly increases the incidence of B cell lymphomas. It remains to be determined how the complex immunologic sequelae that result from these mutations contribute to the transformation process and whether they may be manipulated for therapeutic purposes.

We thank Deirdre Whittaker for expert help with animal breeding and Dr. H.C. Morse for critical reading of the manuscript.

Address correspondence to Dr. Wendy F. Davidson, Department of Immunology, American Red Cross, Holland Laboratory, 15601 Crabbs Branch Way, Rockville, MD 20855. Phone: 301-517-0341; Fax: 301-517-0344; E-mail: davidson@hlsun.redcross.org

Received for publication 10 October 1997 and in revised form 16 March 1998.

References

1. Watanabe-Fukunada, R., C.I. Brannan, N.G. Copeland, N.A. Jenkins, and S. Nagata. 1992. Lymphoproliferation disorder in mice explained by defects in Fas antigen that mediates apoptosis. *Nature*. 356:314–317.
2. Takahashi, T., M. Tanaka, C.I. Brannan, N.A. Jenkins, N.G. Copeland, T. Suda, and S. Nagata. 1994. Generalized lymphoproliferative disease in mice, caused by a point mutation in the Fas ligand. *Cell*. 76:969–976.
3. Adachi, M., R. Watanabe-Fukunaga, and S. Nagata. 1993. Aberrant transcription caused by insertion of an early transposable element in an intron of the Fas antigen gene of *lpr* mice. *Proc. Natl. Acad. Sci. USA*. 90:1756–1760.
4. Suda, T., T. Takahashi, P. Goldstein, and S. Nagata. 1993. Molecular cloning and expression of the Fas ligand, a novel member of the tumor necrosis factor family. *Cell*. 75:1169–1178.
5. Yonehara, S., A. Ishii, and M. Yonehara. 1989. A cell-killing monoclonal antibody (anti-Fas) to a cell surface antigen co-downregulated with the receptor of tumor necrosis factor. *J. Exp. Med*. 169:1747–1756.
6. Trauth, B.C., C. Klas, A.M.J. Peters, S. Matzku, P. Moeller, W. Falk, K.M. Debatin, and P.H. Krammer. 1989. Monoclonal antibody-mediated tumor regression by induction of apoptosis. *Science*. 245:301–304.
7. Suda, T., and S. Nagata. 1994. Purification and characterization of the Fas ligand that induces apoptosis. *J. Exp. Med*. 179: 873–879.
8. Itoh, N., S. Yonehara, A. Ishi, M. Yonehara, S.-I. Mizushima, M. Samechima, A. Hase, Y. Seto, and S. Nagata. 1991. The polypeptide coded by the cDNA for human cell surface antigen Fas can mediate apoptosis. *Cell*. 66:233–243.
9. Cohen, P.L., and R.A. Eisenberg. 1991. *lpr* and *gld*: single

gene models of systemic autoimmunity and lymphoproliferative disease. *Annu. Rev. Immunol.* 9:243–269.
10. Sneller, M.C., S.E. Straus, E.S. Jaffe, J.S. Jaffe, Y.A. Fleisher, M. Stetler-Stevenson, and W.A. Strober. 1992. A novel lymphoproliferative/autoimmune syndrome resembling murine *lpr/gld* disease. *J. Clin. Invest.* 90:334–341.
11. Fisher, G.H., F.J. Rosenberg, S.E. Straus, J.K. Dale, L.A. Middleton, A.Y. Lin, W. Strober, M.J. Lenardo, and J.M. Puck. 1995. Dominant interfering Fas gene mutations impair apoptosis in a human autoimmune lymphoproliferative syndrome. *Cell.* 81:935–946.
12. Rieux-Laucaut, F., F. LeDiest, C. Hivroz, I.A.G. Roberts, K.M. Debatin, A. Fischer, and J.P. de Villartay. 1995. Mutations in Fas associated human lymphoproliferative syndrome and autoimmunity. *Science.* 268:1347–1349.
13. Bettinardi, A., D. Brugnoni, E. Quiros-Roldan, A. Malagoli, S. La Grutta, A. Correra, and L.D. Notarangelo. 1997. Missense mutations in the Fas gene resulting in autoimmune lymphoproliferative syndrome. *Blood.* 89:902–909.
14. Drappa, J., A.K. Vaishaw, K.E. Sullivan, J.-L. Chu, and K.B. Elkon. 1996. *Fas* gene mutations in the Canale-Smith syndrome, an inherited lymphoproliferative disorder associated with autoimmunity. *N. Engl. J. Med.* 335:1643–1649.
15. Davidson, W.F., F.J. Dumont, H.G. Bedigian, B.J. Fowlkes, and H.C. Morse. 1986. Phenotypic, functional, and molecular genetic comparisons of the abnormal lymphoid cells in C3H-*lpr/lpr* and C3H-*gld/gld* mice. *J. Immunol.* 136:4045–4054.
16. Giese, T., and W.F. Davidson. 1995. In $CD8^+$ T cell deficient *lpr/lpr* mice, $CD4^+B220^+$ and $CD4^+B220^-$ T cells replace $B220^+$ double negative T cells as the predominant populations in enlarged lymph nodes. *J. Immunol.* 154:4986–4995.
17. Maldonado, M.A., R.A. Eisenberg, E. Roper, P.L. Cohen, and B.L. Kotzin. 1995. Greatly reduced lymphoproliferation in *lpr* mice lacking major histocompatability complex class I. *J. Exp. Med.* 181:641–648.
18. Mixter, P.F., J.Q. Russell, F.H. Durie, and R.C. Budd. 1995. Decreased $CD4^-CD8^-$ TCR-$\alpha\beta^+$ cells in *lpr/lpr* mice lacking β2 microglobulin. *J. Immunol.* 154:2063–2074.
19. Christianson, G.J., R.L. Blankenburg. T.M. Duffy, D. Panka, J.B. Roths, A. Marshak-Rothstein, and D.C. Roopenian. 1996. Beta-2-microglobulin dependence of the autoimmune syndrome of MRL-lpr mice. *J. Immunol.* 156: 4932–4939.
20. Davidson, W.F., C. Calkins, A. Hugin, T. Giese, and K.L. Holmes. 1991. Cytokine secretion by C3H-*lpr* and -*gld* T cells. Hypersecretion of IFN-γ and tumor necrosis factor-α by stimulated $CD4^+$ T cells. *J. Immunol.* 146:4138–4148.
21. Dumont, F.J., R.C. Habbersett, and L.Z. Coker. 1985. Subsets of Lyt-2 cells defined by differential expression of the 9F3 antigen: alterations in mice of the lpr/lpr genotype. *J. Immunol.* 134:196–203.
22. Giese, T., and W.F. Davidson. 1992. Evidence for early onset, polyclonal activation of T cell subsets in mice homozygous for *lpr*. *J. Immunol.* 149:3097–3106.
23. Budd, R.C., J.H. Schumacher, G. Winslow, and T.R. Mossman. 1991. Elevated production of interferon-γ and interleukin 4 by mature T cells from autoimmune *lpr* mice correlates with Pgp-1 (CD44) expression. *Eur. J. Immunol.* 21: 1081–1084.
24. Reap, E.A., M.L. Piecyk, A. Oliver, E.S. Sobel, T. Waldschmidt, P.L. Cohen, and R.A. Eisenberg. 1996. Phenotypic abnormalities of splenic and bone marrow B cells in *lpr* and *gld* mice. *Clin. Immunol. Immunopath.* 78:21–29.
25. Russell, J.H., B. Rush, C. Weaver, and R. Wang. 1993. Mature T cells of autoimmune *lpr/lpr* mice have a defect in antigen-stimulated suicide. *Proc. Natl. Acad. Sci. USA.* 90:4409–4413.
26. Russell, J.H., and R. Wang, 1993. Autoimmune *gld* mutation uncouples suicide and cytokine/proliferation pathways in activated, mature T cells. *Eur. J. Immunol.* 23:2379–2382.
27. Erikson, J.M., Z. Radic, S.A. Camper, R.R. Hardy, C. Carmack, and M. Weigert. 1991. Expression of anti-DNA immunoglobulin transgenes in non-autoimmune mice. *Nature.* 349:331–334.
28. Roark, J.H., C.L. Kuntz, K.-A. Nguyen, A.J. Caton, and J. Erikson. 1995. Breakdown of B cell tolerance in a mouse model of systemic lupus erythematosus. *J. Exp. Med.* 181: 1157–1167.
29. Rathmell, J.C., and C.C. Goodnow. 1994. Effects of the *lpr* mutation on elimination and inactivation of self-reactive B cells. *J. Immunol.* 153:2831–2842.
30. Marcu, K.B., J. Banerji, N.A. Penncavage, R. Lang, and N. Arheim. 1980. 5′ flanking region of immunoglobulin heavy chain constant region genes displays length heterogeneity in germlines of inbred mouse strains. *Cell.* 22:187–196.
31. Coleclough, C., R.P. Perry, K. Karjalainen, and M. Weigert. 1981. Aberrant rearrangements contribute significantly to the allelic exclusion of immunoglobulin gene expression. *Nature.* 290:372–378.
32. Hedrick, S.M., E.A. Nielson, J. Kavalier, D.L. Cohen, and M.M. Davis. 1984. Sequence relationships between putative T-cell receptor polypeptides and immunoglobulins. *Nature.* 308:153–158.
33. Chattopadhyay, S.K., M.R. Lander, E. Rands, and D.R. Lowy. 1980. Structure of endogenous murine leukemia virus DNA in mouse genomes. *Proc. Natl. Acad. Sci. USA.* 77: 5774–5778.
34. Huppi, K., D. Siwarski, R. Skurla, D. Klinman, and J.F. Mushinski. 1990. *Pvt-1* transcripts are found in normal tissues and are altered by reciprocal (6;15) translocations in mouse plasmacytomas. *Proc. Natl. Acad. Sci. USA.* 87:6964–6968.
35. Jacobson, B.A., D.J. Panka, K.-A. Nguyen, J. Erikson, A.K. Abbas, and A. Marshak-Rothstein. 1995. Anatomy of autoantibody production; dominant localization of antibody-producing cells to T cell zones in Fas-deficient mice. *Immunity.* 3:509–519.
36. Potter, M., and F. Wiener. 1992. Plasmacytomagenesis in mice: model of neoplastic development dependent upon chromosomal translocations. *Carcinogenesis.* 13:1681–1697.
37. Jonkers, J., and A. Berns. 1996. Retroviral insertional mutagenesis as a strategy to identify cancer genes. *Biochem. Biophys. Acta.* 1287:29–57.
38. Stoye, J., and J. Coffin. 1990. Endogenous Viruses. *In* RNA Tumor Viruses. 2nd edition. R. Weiss, N. Teich, H. Varmus, and J. Coffin, editors. Cold Spring Harbor Press, Cold Spring Harbor, NY. 357–404.
39. Phillips, J., K. Mehta, C. Fernandez, and E. Raveche. 1992. The NZB mouse as a model for CLL. *Cancer Res.* 52:437–443.
40. Magrath, I. 1992. Molecular basis of lymphomagenesis. *Cancer Res.* 52(Suppl.):5529–5540.
41. Penn, I. 1986. The occurrence of malignant tumors in immunosuppressed individuals. *Prog. Allergy.* 37:259–300.
42. Morse, H.C., J.W. Hartley, Y. Tang,, S. Chattopadhyay, N. Giese, and T.N. Fredrickson. 1994. Lymphoproliferation as a

precursor to neoplasia: what is a lymphoma? *In* Viruses and Cancer. A. Minson, J. Neil, and M. McCrae, editors. Cambridge University Press. 265–291.
43. Wotherspoon, A.C., C. Ortiz Hidalgo, M.R. Falzon, and P.G. Isaacson. 1991. *Helicobacter pylori*-associated gastritis and primary B-cell gastric lymphoma. *Lancet*. 338:1175–1176.
44. Parsonnet, J., S. Hansen, L. Rodriguez, A.B. Gelb, R.A. Warnke, E. Jellum, N. Orentreich, J.H. Vogelman, and G.D. Friedman. 1994. *Helicobacter pylori* infection and gastric lymphoma. *N. Engl. J. Med*. 330:1267–1271.
45. Peng, S.L., M.E. Robert, A.C. Hayday, and J. Craft. 1996. A tumor-suppressor function for Fas (CD95) revealed in T cell–deficient mice. *J. Exp. Med*. 184:1149–1154.
46. Jelinek, D.F., and P.E. Lipsky. 1987. Enhancement of human B cell proliferation and differentiation by tumor necrosis factor-α and interleukin 1. *J. Immunol*. 139:2970–2976.
47. Finkelman, F.D., I.M. Katona, T.R. Mosmann, and R.L. Coffman. 1988. IFN-γ regulates the isotypes of Ig secreted during in vivo humoral immune responses. *J. Immunol*. 140: 1022–1027.
48. Coffman, R.L., B.W.P. Seymour, D.A. Lebman, D.D. Hiraki, J. Christiansen, B. Shrader, H.M. Cherwinski, H.F.J. Savelkoul, F.D. Finkelman, M.W. Bond, and T.R. Mossman. 1988. The role of helper T cell products in mouse B cell differentiation and isotype regulation. *Immunol. Rev*. 102: 5–30.
49. Go, N.F., B.E. Castle, R. Barrett, R. Kastelein, W. Dang, T.R. Mossman, K.W. Moore, and M. Howard. 1990. Interleukin 10, a novel B cell stimulatory factor: unresponsiveness of X chromosome-linked immunodeficiency B cells. *J. Exp. Med*. 172:1625–1631.
50. Giese, T., J.P. Allison, and W.F. Davidson. 1993. Functionally anergic *lpr* and *gld* $B220^+$ $TcR\alpha/\beta^+$ double negative T cells express CD28 and respond to costimulation with PMA and antibodies to CD28. *J. Immunol*. 151:597–609.
51. Thoman, M.L., and W.O. Weigle. 1989. The cellular and subcellular bases of immunosenescence. *Adv. Immunol*. 46: 221–261.
52. Miller, R.A. 1991. Aging and immune function. *Intl. Rev. Cytol*. 124:187–215.
53. Zhou, T., C.K. Edwards III, and J.M. Mountz. 1995. Prevention of age-related T cell apoptosis defect in CD2-*fas*-transgenic mice. *J. Exp. Med*. 182:129–137.
54. Herndier, B.G., L.D. Kaplan, and M.S. McGrath. 1994. Pathogenesis of AIDS lymphomas. *AIDS* 8:1025–1049.
55. Filipovich, A.H., R. Shapiro, L. Robison, A. Mettens, and G. Frizzera. 1990. Lymphoproliferative disorders associated with immunodeficiency. *In* The Non-Hodgkin's Lymphomas. J.T. McGrath, editor. Arnold Press, London. 135–154.
56. Grufferman, S. 1996. Epidemiology and hereditary aspects of malignant lymphoma and Hodgkin's disease. *In* Neoplastic Diseases of the Blood. Third edition. P.H. Wiernik, G.P. Canellos, J.P. Dutcher, and R.A. Kyle, editors. Churchill Livingstone, New York.737 pp.
57. Morse, H.C., S. Chattopadhyay, M. Makino, T.N. Fredrickson, A.W. Hugin, and J.W. Hartley. 1992. Retrovirus-induced immunodeficiency in the mouse: MAIDS as a model for AIDS. *AIDS* 6:607–621.
58. Tang, Y., S. Chattopadhyay, J.W. Hartley, T.N. Fredrickson, and H.C. Morse. 1994. Clonal outgrowths of T and B cells in *scid* mice reconstituted with cells from mice with MAIDS. *In Vivo*. 8:953–960.
59. Radl, J. 1990. Age-related monoclonal gammopathies: clinical lessons from the aging C57BL mouse. *Immunol. Today*. 11:234–236.
60. Radl, J., Y. Punt, M.H. van den Enden-Vieveen, P. Bentvelzen, M.H.C. Bakkus, Th.W. van den Akker, and R. Benner. 1990. The 5T mouse multiple myeloma model: absence of *c-myc* oncogene rearrangement in early transplant generations. *Br. J. Cancer*. 61:276–278.
61. Lin, A., J. Dale, T. Fleisher, G. Fisher, F. Rosenberg, M. Lenardo, J. Puck, L. Middleton, B. Corden, M. Tucker, and S. Straus. 1995. Familial aggregation of Hodgkin's disease (HD), and autoimmune lymphoproliferative syndrome (ALPS) and germline Fas mutations. *Blood*. 86(Suppl. 1):271*a*. (Abstr.)
62. Landowski, T.H., N. Qu, I. Buyuksal, J.S. Painter, and W.S. Dalton. 1997. Mutations in the Fas antigen in patients with multiple myeloma. *Blood*. 90:4266–4270.
63. Zornig, M., A. Grzeschiczek, M-B. Kowalski, K.-U. Hartmann, and T. Moroy. 1995. Loss of Fas/Apo-1 receptor accelerates lymphomagenesis in *Eμ-myc* transgenic mice but not in animals infected with MoMuLV. *Oncogene*. 10:2397–2401.
64. Moroy, T., A. Grzesschiczek, S. Petzold, and K.-U. Hartman. 1993. Expression of a *pim-1* transgene accelerates lymphoproliferation and inhibits apoptosis in *lpr/lpr* mice. *Proc. Natl. Acad. Sci. USA*. 90:10734–10738.
65. Peters, R.L., L.S. Rabstein, R.M. Spahn, R.M. Madison, and R.J. Huebner. 1972. Incidence of spontaneous neoplasms in breeding and retired breeder BALB/cCr mice throughout the natural lifespan. *Int. J. Cancer*. 10:273–282.
66. Akamatsu, Y., and B.P. Barton. 1974. Neoplasms and amyloidosis in strains of mice treated with 3-methylcholanthrene. *J. Natl. Cancer Inst*. 52:377–385.
67. Morse, H.C. III, J.B. Roths, W.F. Davidson, W.Y. Langdon, T.N. Fredrickson, and J.W. Hartley. 1985. Abnormalities induced by the mutant gene, *lpr*. Patterns of disease and expression of murine leukemia viruses in SJL/J mice homozygous and heterozygous for *lpr*. *J. Exp. Med*. 161:602–616.